*Proceedings of the 21st ICSMGE, Vienna, Austria, 14 – 19 June 2026. Pistrol, Adam & Schweiger (eds.)*
*Published by: ÖGG, Austrian Society for Geomechanics, Salzburg, Austria, ISBN 978-3-9503898-4-5*
*https://doi.org/10.53243/ICSMGE2026-1381*

# Liquefiable soils in the Sakarya region and their effects on settlement criteria of structures

**Hande Yumuk Ceylan,** Hidayet Kemal Uyar, Emel Sıkıcı, Hilmi Turan Durgunoglu
*Geotechnical Department, Zemin Etud ve Tasarim A.S., Istanbul, Türkiye, hande.yumuk@zeminas.com.tr*

Sadık Oztoprak
*Department of Civil Engineering, İstanbul University, Türkiye*

ABSTRACT: Geological and geophysical investigations conducted since 2010 in the industrial facility area located in the Sakarya Province have revealed that the site exhibits liquefiable soil characteristics under large-magnitude earthquakes. Comprehensive studies, including SPT, CPT, MASW, PS Logging, laboratory tests, and other fieldwork, have clearly demonstrated the soil's liquefaction potential. Given the soil characteristics, seismic activities, and high groundwater levels, understanding the impact of liquefaction effects on the foundations of structures built in susceptible areas is a critical issue. Although the foundations of existing structures in the region have been improved using methods based on outdated codes, the potential for liquefaction-induced settlements remains a significant threat. In this context, assessing the settlements caused by liquefaction in accordance with the architecture and settlement criteria of existing structures is essential. This study focuses on the industrial facility site in Sakarya and analyzes the settlements caused by liquefaction effects using Deep Soil 1D and Plaxis 2D analyses. These analyses incorporate bedrock depth and dynamic parameters determined through advanced geophysical methods (e.g., SPAC) to derive site-specific ground motion spectra required for structural analyses. The study aims to investigate the impacts of liquefaction on the architectural and settlement behavior of the structures. Predicting liquefaction-induced settlements is a critical finding for ensuring the longevity and safety of structures. Recommendations have been provided to enhance the durability and earthquake resilience of existing structures through additional methods. The results of this study serve as a guide for future soil improvement projects in the area.

KEYWORDS: Liquefiable soils, Probabilistic Seismic Hazard Analysis (PSHA), Site Response Analysis (SRA), Design Acceleration Spectrum

## 1 INTRODUCTION

Sakarya Province, located in northwestern Türkiye, lies within the influence zone of the North Anatolian Fault Zone (NAFZ)—one of the world's most active and well-documented strike-slip fault systems. The NAFZ accommodates the right-lateral motion between the Anatolian and Eurasian plates with a slip rate of 20–25 mm/year. The region has experienced numerous destructive earthquakes throughout history, most notably the 1999 Kocaeli earthquake (Mw 7.4), which caused extensive soil liquefaction and severe damage to both industrial and residential structures.

The study area is situated in the Adapazarı Plain; a tectonically controlled subsidence basin filled with thick Quaternary alluvial and deltaic deposits. These deposits, commonly exceeding 30–40 m in thickness, consist of loose to medium-dense silty sands, sandy silts, and clay lenses, underlain by older lacustrine and alluvial fan sediments. Borehole and geophysical surveys indicate basin depths exceeding 100 m in certain locations, while groundwater is typically encountered within 1–3 m of the surface. Such geological and hydrogeological conditions create a high liquefaction potential under strong ground shaking.

The concentration of industrial facilities in the region makes the consequences of earthquake-induced liquefaction particularly severe, extending beyond structural damage to include production downtime, environmental hazards, and major economic losses. Although some facilities have undergone ground improvement, many interventions were carried out under outdated seismic codes and may not meet current performance requirements.

In this context, the present study investigates the liquefaction potential and associated settlement behavior of an industrial facility site in Sakarya Province. A comprehensive program of field and laboratory investigations—including SPT, CPT, MASW, PS Logging, and SPAC methods—was integrated with advanced geotechnical analyses. Site-specific ground motion inputs derived from probabilistic and deterministic seismic hazard assessments were applied in DEEPSOIL 1D and PLAXIS 2D models. The study aims to quantify liquefaction-induced settlements, assess their impact on the performance of existing structures, and propose improvement measures to enhance the seismic resilience of the facility.

## 2 NEOTECTONIC FRAMEWORK AND SEISMICITY

Located in a seismically active sector of northwestern Türkiye, the Adapazarı Plain lies near the Geyve–Sapanca and Karadere fault segments of the North Anatolian Fault Zone (NAFZ), one of the most prominent and active strike-slip fault systems in the world. This tectonic position makes the region susceptible to the effects of large-magnitude (Mw > 7.0) earthquakes originating from relatively short distances.

The physical characteristics and tectonic framework of the region are critical for identifying applicable Ground Motion Prediction Equations (GMPEs) and selecting stochastic models to be used in probabilistic seismic hazard analyses. Turkey's general neotectonics framework comprises 18 seismotectonic regions (Figure 1).In this context, the project site in Sakarya is located between the Eastern Marmara and Western Black Sea regions, within the influence of the North Anatolian Fault Zone (NAFZ), which accommodates the relative motion between the Eurasian Plate and the Anatolian Block.

While most of the fault segments considered in the seismic hazard assessment for the site belong to the NAFZ seismotectonic region, additional seismic sources include the reverse fault system forming the southern boundary of the Black Sea Basin to the north, and the Eskişehir and İnegöl fault zones in Central Anatolia to the south. No active fault has been identified within 25 km of the project site.

Among the tectonic structures contributing to the region's seismic hazard, the faulting that forms the Western Black Sea Basin exhibits low recorded seismicity, with no documented or inferred earthquakes of magnitude M > 6.0 and overall low activity, based on the historical earthquake catalog compiled within the "Revision of the Turkish Seismic Hazard Map"(Figure 2).

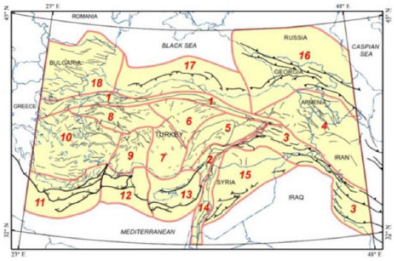


Figure 1. Tectonic regions of Turkey and its surroundings (Duman et al., 2018).

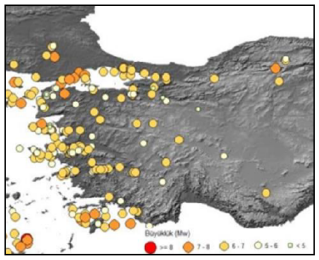

Figure 2. Historical period earthquakes in Western Turkey (modified from Akkar et Al., 2014).

The primary seismic hazard for the study area arises from the NAFZ. Following the 1912 earthquake on the Ganos Fault, a westward earthquake migration has been observed along the NAFZ since 1939, culminating most recently in the 1999 İzmit and Düzce earthquakes.

After more than a century of progressive rupture, several segments along the NAFZ remain unbroken, including the Adalar, Kumburgaz, and Silivri segments on the northern branch in the Marmara Sea, and the İznik, Geyve, and Gemlik segments on the southern branch, all of which are considered seismic gaps with potential for future large events.

## 3 SOIL PROFILE AND LIQUEFACTION RISK

### 3.1 *Soil Investigation*

Considering the expected soil conditions at the site, an investigation program comprising borehole drilling, Standard Penetration Tests (SPT), Cone Penetration Tests (CPTu), Seismic Cone Penetration Tests (SCPTu), collection of undisturbed and representative samples, groundwater level measurements, pressuremeter tests, and geophysical surveys (MASW, microtremor, Electrical Resistivity [DES], Electrical Resistivity Tomography [ERT], PS Logging, and Spatial Circular Array Microtremor [SPAC]) has been cumulatively carried out by different companies in the investigation area and its surroundings from 2010 to the present (Table 1 and Table 2).

Table 1. Geotechnical investigations.

| Test Type | Number of Tests | Test Type |
|---|---|---|
| Borehole Drilling | 98 (max depth 80 meters) | Borehole Drilling |
| CPT / CPTu | 18 (max depth 23.14 meters) | CPT / CPTu |
| SCPTu | 4 (max depth 23.54 meters) | SCPTu |

Table 2. Geophysical investigations.

| Test Type | Total Number | Test Type |
|---|---|---|
| MASW–Seismic Refraction | 49 | MASW–Seismic Refraction |
| Microtremor | 8 | Microtremor |
| Resistivity (DES / ERT) | 4 | Resistivity (DES / ERT) |

### 3.2 *Soil Profile*

In all boreholes drilled within the investigation area, Quaternary-aged Alluvium (Qal) units were encountered, consisting of heterogeneous and gradational deposits of silt, clay, sand, and gravel sizes. It was observed that the alluvial units are unconsolidated, the soil lithology varies over short distances, and the layer boundaries are indistinct. Details regarding the soil units identified within the investigation area are presented in Figure 3 and Table 3, while the shear wave velocity of these alluvial deposits varying with depth is shown in Figure 4.

Table 3. Idealized Soil Parameters

| Layer | Thickness (m) | $SPTN_{30}$ | ϕ° | Vs,ort (m/s) | Plasticity Index IP |
|---|---|---|---|---|---|
| Clayey Gravelly Sand | 12.5 | 8-15 | 30-32 | 138-210 | NP-12 |
| Sandy Gravel | 8 | 25 | 34 | 225-245 | NP |
| Sandy Gravelly Clay | 22.5 | 25-40 | - | 255-335 | 10-15 |
| Sandy Silty Gravel | 15 | 30-50 | 34-36 | 350 | NP |
| Gravelly Silty Sand | 9.5 | 60 | 36 | 370-420 | NP-10 |
| Sandy Silt | 9.5 | 50 | 36 | 420-455 | NP-8 |
| Clay | 43 | 60-R | | 478-635 | 12 |
| Bedrock | - | | | 760 | - |

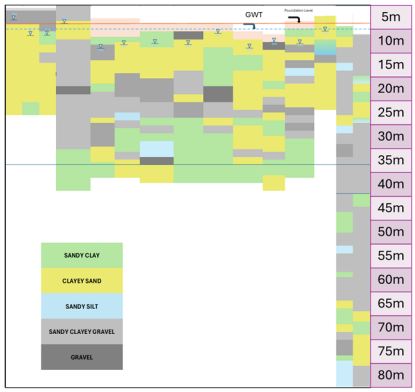


Figure 3. Soil profile.

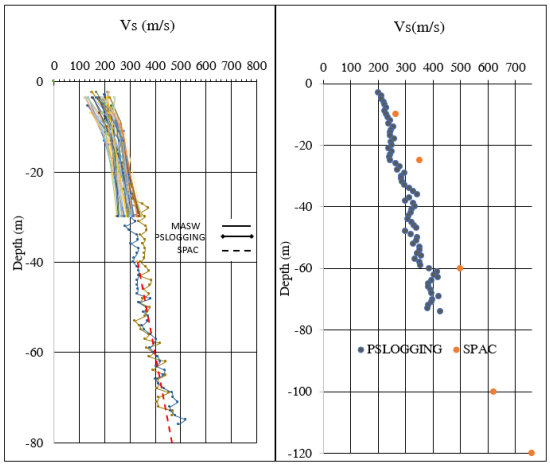


Figure 4. Shear wave velocity profile based on downhole, surface and deep geophysical investigations.

### 3.3 *Liquefaction Analyzes (Based on SPT and CPT)*

Based on the geological–geomorphological structure and climatic characteristics of the investigation area, the most significant natural hazard expected is earthquakes. According to the Turkey Earthquake Hazard Map, the investigation area is located in a region with high seismic risk and is influenced by the North Anatolian Fault Zone (NAFZ). The project site is situated approximately 1.0 km from the nearest Dokurcun Segment, 2.5 km from the Karadere Segment, and about 5.0 km from the Arifiye Segment of the NAFZ.

The project area and its surroundings are surrounded by active fault zones capable of generating destructive earthquakes; therefore, the site is located in a high seismic risk region. Given its proximity to the North Anatolian Fault Zone, the project site is expected to be significantly affected—resulting in potential loss of life and property—by earthquakes of magnitude 6.5 or greater that may occur on this fault.

In this study, the moment magnitude (Mw) employed for the deterministic seismic hazard scenario was derived from a full model deaggregation of the underlying PSHA framework, conducted in accordance with the procedures of ASCE 7-16. The deaggregation results indicate that the controlling seismic source corresponds to an effective moment magnitude of Mw = 8.05 and amax=0.87.

According to SPT- and CPT-based assessments consistently indicated the presence of liquefaction-susceptible layers within the project site, highlighting the need to evaluate ground improvement alternatives (Figure 5).

#### 3.3.1 *SPT-Based Analyses:*

In accordance with Section 16 of Turkish Building Earthquake Code (TBEC-2018), SPT blow counts were corrected for fines content ($N_{1,60f}$), and the cyclic resistance ratio ($CRR_{7.5}$) was determined. The magnitude scaling factor ($C_M$) was applied to derive liquefaction resistance ($\tau_R$).

The cyclic shear stress induced by the earthquake ($\tau$earthquake) was calculated using the short-period spectral acceleration coefficient, $S_{DS}$ = 1.926. Results indicated that gravelly sand/silty sand layers located below the groundwater table exhibited safety factors (GF) against liquefaction of less than 1.10, indicating liquefaction potential. The maximum depth at which liquefaction-susceptible layers were identified was 19.50 meters depth.

#### 3.3.2 *CPT-Based Analyses:*

Liquefaction resistance was determined directly from corrected cone tip resistance ($q_{c1Ncs}$) using the Robertson and Fear (1997) method. Magnitude scaling factors (MSF = 102.24 / $Mw^{2.56}$) were applied to compute safety factors (GF) for different earthquake magnitudes.

CPT results confirmed the SPT-based findings, indicating liquefaction potential in sandy-silty layers below the groundwater table.

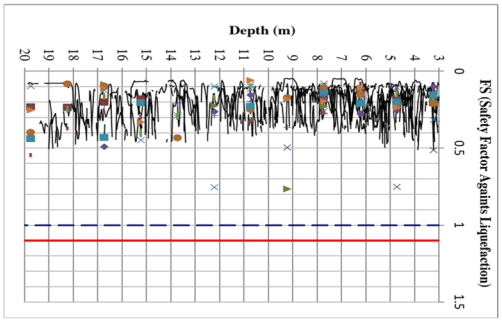


Figure 5. Liquefaction potential analyses.

## 4 PROBABLISTIC SEISMIC HAZARD ASSESMENT (PSHA)

Probabilistic seismic hazard analyses for the project site were conducted using a combination of specialized software and toolkits, including ZMAP7 (Weimer, 2001) operating in MATLAB, the OpenQuake engine (Pagani et al., 2014) developed by the GEM (Global Earthquake Model) Foundation, and its associated Python-based libraries—HMTK (Hazard Modeller's Toolkit), SMTK (Strong Motion Toolkit), and MBTK (Model Builder's Toolkit). All hazard computations were ultimately carried out within the OpenQuake framework.

The background seismicity mapped faults in the study area, seismic source models/parameters, and selected ground motion prediction equations (GMPEs) were defined within the software. To account for epistemic uncertainties in both seismic source modeling and GMPE selection, a logic-tree approach was implemented. Equal-hazard spectra and spectral parameters were computed for both rock outcrop (site-independent) and site-specific conditions based on $Vs_{30}$ values.

The resulting spectrum was compared with the design spectrum recommended by TBEC-2018 for the project site, and an envelope spectrum was developed to derive site-specific horizontal and vertical elastic acceleration spectra.

The development of seismic source models was based primarily on the "European Seismic Hazard Map 2020" (ESHM20) presented by Danciu et al. (2021) and on datasets/models compiled within the "Updating the Turkish Seismic Hazard Map" project (UDAP-Ç-13-06; Akkar et al., 2014) conducted under the National Earthquake Research Program (UDAP). Accordingly, four alternative source models were incorporated into the hazard assessment—two area-source models, one fault-source model, and one combined fault + spatially smoothed seismicity model—together with four different GMPEs, all integrated through the logic-tree framework.

### 4.1 *Seismic Source Modeling Approach*

In this study, four seismic source models were developed within three distinct modeling approaches to address epistemic uncertainties in the probabilistic seismic hazard assessment: two area source models (ASM1, ASM2), one fault source model (FSM), and one combined fault + spatially smoothed seismicity model (F+SSM). Area sources are defined within boundaries determined by factors such as seismicity distribution, fault characteristics, and geology, assuming homogeneous seismic activity within each zone. Fault sources are modeled individually based on the geometry and seismotectonic parameters of each mapped fault. The spatially smoothed seismicity model distributes seismicity according to observed activity density, rather than homogeneously, and was combined with the fault source model in this study to represent background seismicity not directly associated with mapped faults.

### 4.2 *Applied Relationships and Parameters*

Seismic source models were implemented using the internal definitions available in the OpenQuake software. The model parameterization employed the truncated Gutenberg–Richter magnitude–recurrence relationship, the Wells and Coppersmith (1994) surface rupture area–magnitude scaling relationship, and the Jayaram and Baker (2009) ground-motion correlation model. By integrating alternative source definitions and uncertainty parameters through the logic-tree framework, more robust and site-representative seismic hazard estimates were obtained for the project site.

### 4.3 *Ground Motion Prediction Equations (GMPEs)*

For the project site, candidate GMPEs were selected from widely used regional and global models applicable to Turkey, including both recent and well-established formulations. Special consideration was given to studies following the 6 February 2023 Pazarcık earthquake. Among the selected models, Kotha et al. (2022; KWBC22) is the most recent, developed using the European strong-motion database with significant inclusion of Turkish records; Kale et al. (2015; KAAH15) is a regional model derived from the Turkish strong-motion database; Chiou and Youngs (2014; CY14) and Boore et al. (2014; BSSA14) are NGA-West2 models based on global shallow active crustal events, with the latter incorporating an anelastic attenuation term to capture regional effects in Turkey. Akkar et al. (2014; ASB14) provides a model for Europe, the Mediterranean, and the Middle East.

### 4.4 *PSHA Analyzes Result*

According to the results obtained for the surface unit, the analysis spectra exhibit higher values than those specified by TBEC-2018 in the short-period range for DD2 and DD3 earthquake levels, and across all earthquake levels at a period of 1.0 second. The comparison of the acceleration spectra calculated through probabilistic seismic hazard analysis for the project site's base unit ($Vs_{30}$ = 221 m/s) with the TBEC-2018 spectrum for soil class ZD is presented in Figure 8 and Table 4.

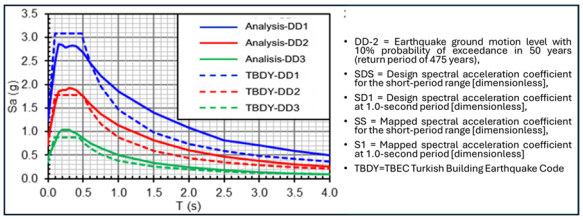


Figure 6. Probabilistic seismic hazard analysis for the $Vs_{30}$ = 221m/s versus the TBEC-2018 spectrum for soil class ZD.

Table 4. Spectral parameter comparison between PSHA results for $VS_{30}$ = 251 m/s and TBEC-2018 ZD site class.

| Spectra | $S_{DS}$ (g) | $S_{D1}$(g) |
|---|---|---|
| Ground Motion | DD2 | DD2 |
| TBEC-ZD | 1.773 | 0.874 |
| PSHA | 1.926 | 1.129 |

### 4.5 *PSHA Design Spectra*

The horizontal acceleration spectrum obtained from the hazard analysis was generated in terms of the geometric mean (GM) of the horizontal components. The selected ground motion prediction equations (GMPEs) do not account for near-fault effects such as orientation or directivity. However, the nearest active fault to the study area is located approximately 5 km away, and the region is surrounded by faults within 25 km. Therefore, following the recommendations of CALTRANS (2019), a near-fault correction was applied to the "Analysis Spectrum" to obtain the "Design Spectrum," resulting in a "Corrected Spectrum".

The earthquake records requested within the scope of this study will be spectrally matched to the geometric mean spectrum—applied at the base of the two-dimensional geotechnical model—using a one-dimensional full matching method, and to 1.3 times this spectrum for the three-dimensional case, using a spectral matching approach. Considering the specified requirements and methods, the necessary horizontal elastic "Design Spectra" were defined as the envelope of the "Corrected Spectrum" and the TBEC-2018 spectrum. The "Vertical Design Spectrum" was calculated in accordance with TBEC-2018 provisions, based on the derived "Design Spectrum" (Figure 7).

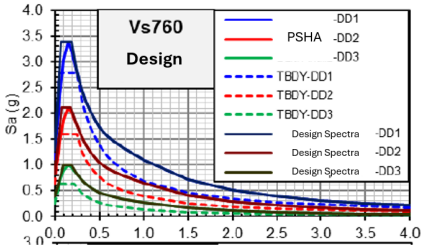


Figure 7. PSHA design spectra vs TBEC (AFAD).

## 5 SITE RESPOSE ANALYZES (SRA)

For the industrial facility site, SPAC measurements and seismic hazard analysis results indicated that the engineering bedrock is located at a depth of approximately 120 m. Based on these findings, an idealized soil profile extending from the ground surface to this depth was developed for use in site-specific 1D ground response analyses. All soil behavior assessments were performed for the DD-2 earthquake level in accordance with TBEC 2018 provisions.

### 5.1 *1D Site Response Analysis*

The nonlinear behavior of soils depends on both inherent material properties and earthquake loading characteristics. For long-duration, high-magnitude shaking, nonlinear effects become more pronounced, with stiffness degradation occurring due to cyclic stress–strain behavior. In saturated soils, excess pore water pressure-buildup can further soften the soil, increasing deformation demands. Accurately capturing these mechanisms requires the application of nonlinear constitutive models.

Site investigations confirmed the presence of Deep Soil Mixing (DSM) columns only beneath the foundation footprint, with no improvement beneath floor slabs. Accordingly, three alternative scenarios were analyzed: maximum improvement ratio beneath the foundation, no improvement, improvement within the top 10 m beneath slabs. For each case, site-specific response spectra were developed and compared (Figure 8 and Figure 9).

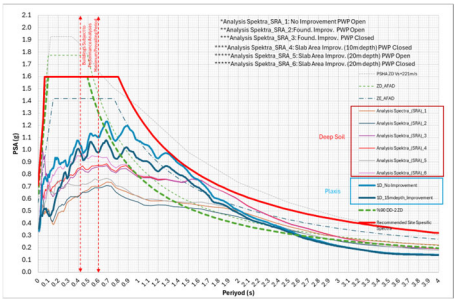


Figure 8. Recommended foundation level spectra based on 1D analysis.

Following TBEC 2018 Section 16.5.1.2, a one-dimensional, horizontally layered free-field soil profile was modeled for dynamic response analyses. Shear strain evaluations performed under Section 16.5.2.2(b) provisions revealed threshold shear strains exceeding 1%, necessitating the use of a nonlinear time-domain approach rather than the equivalent-linear method. The dynamic soil model was terminated at the engineering bedrock layer, with a shear wave velocity (Vs) of 760 m/s.

In accordance with TBEC 2018 Section 16.5.2.3(c), the soil column was discretized into 55 sublayers, ensuring that the highest frequency represented did not exceed 25 Hz. The General Quadratic/Hyperbolic (GQ/H) model was adopted in DEEPSOIL to simultaneously represent both the initial shear modulus at small strains and limiting shear strength at large strains. Hysteretic damping behavior was modeled using non-Masing rules, and modulus reduction and damping curves were corrected using the Darendeli MRDF approach.

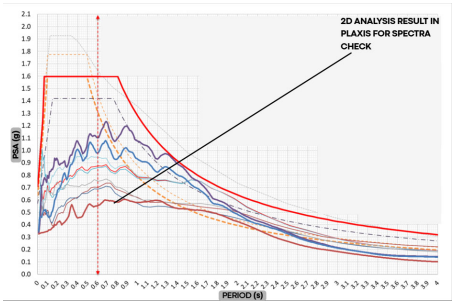


Figure 9. Recommended foundation level spectra based on 1D and 2D analysis.

### 5.2 *2D Site Response Analysis*

Complementary 2D coupled dynamic–consolidation analyses were performed using PLAXIS 2D v2024 with the liquefiable soil model PM4Sand to assess potential post-earthquake settlement due to liquefaction. Boundary conditions included a Compliant Base for horizontal limits and Tied Degrees of Freedom elements in 1D simulations to model vertical wave propagation. In 2D simulations, Free Field boundaries were adopted to simulate realistic lateral energy dissipation.

Seismic input consisted of 11 acceleration time histories, applied as prescribed displacements at the model base. The analyses were conducted for both the existing foundation configuration and the considered improvement scenarios, with a focus on evaluating potential liquefaction-induced settlements within the project site.

#### 5.2.1 *Constitutive Models*

For the liquefiable soil layers identified at the site, dynamic analyses were performed in PLAXIS 2D using both the Hardening Small Strain and PM4Sand constitutive models. The model depth was defined as 125 m in total, comprising the 120 m soil profile determined from site investigations and a 5 m elastic base layer, excluding the building height. This depth was considered sufficient for dynamic simulations, as the horizontal dampers at the base operate numerically with high efficiency. The Free Field absorbing boundaries can reflect incident waves arriving at angles narrower than approximately 30°, and for a conservative approach using a 45° criterion, the model needs to be extended laterally by at least its depth (125 m). Accordingly, the modeled cross-section length was approximately 133 m, with a total model width of 600 m.

The PM4Sand constitutive model can simulate excess pore water pressure generation and post-liquefaction volumetric reconsolidation in sands under cyclic loading. The model is based on a stress-ratio–controlled, critical state compatible, bounding surface plasticity formulation (Manzari and Dafalias, 1997; Dafalias and Manzari, 2004) and is implemented in Plaxis as version 3.2 (Boulanger and Ziotopoulou, 2022).

The soil profile was idealized based on Cone Penetration Test (CPT) data, and the PM4Sand model was calibrated for the liquefiable layers identified. The primary reason for selecting this model was its proven capability to accurately capture post-liquefaction deformation and settlement behavior in sandy soils.

For the liquefiable layers, the SPT- and CPT-based CRR–N curves determined from site-specific analyses were used as reference targets for the PM4Sand model calibration, with greater emphasis placed on the CPT-derived curves during the process. The calibration procedure began by keeping all parameters at their default values, followed by calculating Dr and $G_o$ from field test data, and subsequently calibrating the hpo parameter.

The $h_{po}$ calibration was performed by identifying the value that, under the shear stress corresponding to the target CRR at N = 15 in the reference curve, resulted in 3% shear strain being reached in exactly 15 loading cycles (Quevedo, 2019). The CRR values used in the target curves were computed using the approach of Boulanger and Idriss (2014), while the corresponding N values were derived from the empirical relationship between earthquake magnitude (Mw) and the equivalent number of significant stress cycles (N) proposed by Kramer (1996).

To determine the timing for activating the "PostShake" switch parameter of the PM4Sand model, the point at which each earthquake record reached 95% of its cumulative Arias Intensity was identified.

### 5.3 *Liquefaction Settlement Based on 2D SRA*

According to the analysis results, along the depth range predicted to undergo liquefaction, the pore water pressure ratios were found to reach $r_{u,max} \geq 1.0$ particularly within the Z2 and Z3 layers. In the analysis, the Z1 layer remained above the groundwater level but approached $r_{u,max} \approx 0.7$ due to the influence of volumetric displacements occurring in the underlying layers (Figure 10).

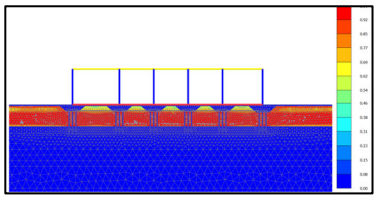

Figure 10. Pore water pressure ratio.

The applied lateral forces caused notable deformations in the outer foundations, as well as differential settlements and swelling within the foundation system. The displacements reported herein are solely attributable to liquefaction-induced behavior during the earthquake and do not include settlements that occurred under construction stages or building loads modeled in the initial phases of the analysis.

Assuming that the settlement limits for isolated footings were exceeded, the building section analyzed—shown in Figure 11—was re-analyzed by interconnecting the foundations with earthquake beams to mitigate differential movements. In the existing condition, the foundations are connected with beams only in one direction. For the revised scenario, earthquake beams with dimensions 30 cm × 50 cm were modeled. The analysis results indicated that the addition of these beams significantly, approximately %40, constrained foundation rotations (Table 5).

Table 5. Differential settlements.

| Average Earthquake | Singular Foundation Maximum Differential Settlement of Edges (mm) |
|---|---|
| Without Beams | *18.0* |
| With Beams | *7.0* |

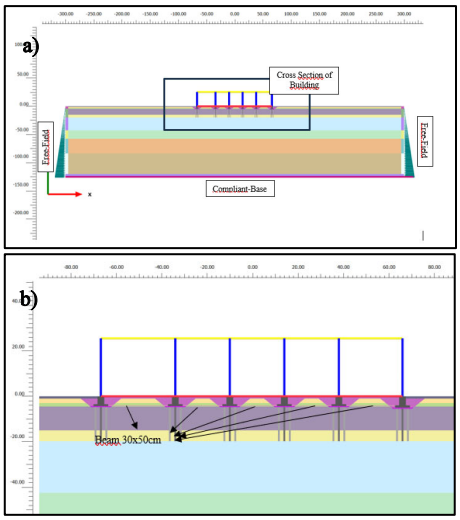

Figure 11. 2D analysis models a) current situation b) the case with tie beams added.

## 6 CONCLUSIONS

The findings of this study highlight the significant liquefaction potential of the Adapazarı Plain, where industrial facilities are founded on thick, unconsolidated alluvial deposits with shallow groundwater conditions. While earlier ground improvement measures were implemented based on outdated seismic codes, current analyses indicate that liquefaction-induced settlements remain a critical risk for existing structures.

Numerical simulations performed with DEEPSOIL (1D) and PLAXIS 2D (PM4Sand model) confirmed that excess pore water pressure generation and cyclic mobility can induce considerable foundation deformations, particularly within sandy–silty soil layers. Differential settlements and rotations were observed in the existing foundation configuration. The introduction of tie beams significantly reduced these effects, demonstrating the importance of structural mitigation in addition to soil improvement.

For the operational industrial facility considered in this study, injections beneath slab areas and bidirectional interconnection of isolated footings are recommended as practical and effective countermeasures. More broadly, the results emphasize that reliable liquefaction assessments and site-specific response analyses are essential for the seismic safety of critical infrastructure in the Sakarya region. These findings provide guidance for upgrading existing facilities and designing future soil improvement strategies in liquefaction-prone areas.

## 7 ACKNOWLEDGEMENTS

The authors would like to express their sincere gratitude to all the dedicated staff of Zemin Etüd ve Tasarım A.Ş. for their profound knowledge and commitment to research. Their expertise in geotechnical engineering, continuous technical support, and dedication to quality played a critical role in the successful completion of this project.

## 8 REFERENCES

Akkar, S., Çagnan, Z. & Yenier, E. 2014. Revision of the Turkish seismic hazard map: New ground motion models and updated source characterization. Final Report, Project UDAP-Ç-13-06, National Earthquake Research Program (UDAP). AFAD, Ankara.

Akkar, S., Özen, O. & Cultrera, G. 2014. Ground-motion models for the Turkish region: Historical and recent earthquake records. Bulletin of Earthquake Engineering, 12(1), pp. 1–36.

Akkar, S., Sandıkkaya, M.A. & Bommer, J.J. 2014. Empirical ground-motion models for point- and extended-source crustal earthquake scenarios in Europe and the Middle East. Bulletin of Earthquake Engineering, 12, pp. 359–387.

ASCE. 2017. ASCE/SEI 7-16: Minimum Design Loads and Associated Criteria for Buildings and Other Structures. Reston, VA: American Society of Civil Engineers.

Boore, D.M., Stewart, J.P., Seyhan, E. & Atkinson, G.M. 2014. NGA-West2 equations for predicting PGA, PGV, and 5% damped spectral accelerations. Earthquake Spectra, 30, pp. 1057–1085.

Boulanger, R.W. & Idriss, I.M. 2014. CPT and SPT Based Liquefaction Triggering Procedures. Report No. UCD/CGM-14/01. University of California, Davis.

Boulanger, R.W. & Ziotopoulou, K. 2022. PM4Sand (Version 3.2): A Sand Plasticity Model for Earthquake Engineering Applications. Report No. UCD/CGM-22/02, July.

CALTRANS. 2019. CALTRANS Seismic Design Criteria v2.0. State of California Department of Transportation.

Chiou, B.S.-J. & Youngs, R.R. 2014. Update of the Chiou and Youngs NGA ground-motion model for shallow crustal earthquakes. Earthquake Spectra, 30, pp. 1117–1153.

Dafalias, Y.F. & Manzari, M.T. 2004. Simple plasticity sand model accounting for fabric change effects. Journal of Engineering Mechanics, 130(6), pp. 622–634.

Danciu, L., Garcia, J., Şeşetyan, K., Basili, R., Poggi, V., Rovida, A. et al. 2021. The 2020 European Seismic Hazard Model (ESHM20). Bulletin of Earthquake Engineering, 19, pp. 1–66.

Darendeli, M.B. 2001. Development of a New Family of Normalized Modulus Reduction and Material Damping Curves. PhD Dissertation. University of Texas at Austin.

Duman, T.Y., Emre, Ö. & Özalp, S. 2018. Active Fault Map of Turkey and Its Surroundings. General Directorate of Mineral Research and Exploration (MTA), Ankara.

Hardin, B.O. & Drnevich, V.P. 1972. Shear modulus and damping in soil: Design equations and curves. Journal of the Soil Mechanics and Foundations Division, 98(7), pp. 667–692.

Jayaram, N. & Baker, J.W. 2009. Correlation model of spectral acceleration values. Earthquake Engineering and Structural Dynamics, 38, pp. 1687–1708.

Kale, Ö., Akkar, S., Alavi, A.H. & Hamzehloo, H. 2015. A set of ground-motion prediction equations for shallow crustal earthquakes in Turkey. Bulletin of Earthquake Engineering, 13, pp. 249–275.

Kotha, S.R., Weatherill, G.A., Bindi, D. & Cotton, F. 2022. A regionally adaptable ground-motion model for Europe and the Middle East. Bulletin of Earthquake Engineering, 20, pp. 1673–1700.

Kramer, S.L. 1996. Geotechnical Earthquake Engineering. Upper Saddle River, NJ: Prentice Hall.

Manzari, M.T. & Dafalias, Y.F. 1997. A critical state two-surface plasticity model for sands. International Journal for Numerical and Analytical Methods in Geomechanics, 21, pp. 611–636.

Pagani, M., Monelli, D., Weatherill, G., Danciu, L., Crowley, H., Silva, V., Henshaw, P. et al. 2014. OpenQuake engine: An open hazard and risk software for the Global Earthquake Model. Seismological Research Letters, 85, pp. 692–702.

PLAXIS. 2024. PLAXIS 2D Reference Manual. Bentley Systems International Limited, Dublin.

Quevedo, L. 2019. Calibration of the hpo Parameter for PM4Sand Based on Target CRR–N Relationships. M.S. Thesis, University of California, Davis.

Robertson, P.K. & Fear, C.E. 1997. Liquefaction of sands and its evaluation. In: Proceedings of the 1st International Conference on Earthquake Geotechnical Engineering, Tokyo, Japan, pp. 125–132.

Seed, H.B. & Idriss, I.M. 1970. Soil Moduli and Damping Factors for Dynamic Response Analyses. Technical Report EERC-70-10. University of California, Berkeley.

Turkish Building Earthquake Code (TBEC-2018). 2018. Disaster and Emergency Management Authority (AFAD), Ankara.

Weimer, S. 2001. ZMAP—A toolbox for analyzing seismicity patterns. Computers & Geosciences, 27, pp. 441–446.

Wells, D.L. & Coppersmith, K.J. 1994. New empirical relationships among magnitude, rupture length, rupture width, rupture area, and surface displacement. Bulletin of the Seismological Society of America, 84, pp. 974–1002.